Structural Determinants of Gating in Inward-Rectifier K^+ Channels

Han Choe,* Lawrence G. Palmer,* and Henry Sackin#

*Department of Physiology and Biophysics, Cornell University Medical College, New York, New York 10021, and #Department of Physiology and Biophysics, The Chicago Medical School, North Chicago, Illinois 60064 USA

ABSTRACT The gating characteristics of two ion channels in the inward-rectifier K^+ channel superfamily were compared at the single-channel level. The strong inward rectifier IRK1 (Kir 2.1) opened and closed with kinetics that were slow relative to those of the weakly rectifying ROMK2 (Kir 1.1b). At a membrane potential of −60 mV, both IRK and ROMK had single-exponential open-time distributions, with mean open times of 279 ± 58 ms ($n = 4$) for IRK1 and 23 ± 1 ms ($n = 7$) for ROMK. At −60 mV (and no EDTA) ROMK2 had two closed times: 1.3 ± 0.1 and 36 ± 3 ms ($n = 7$). Under the same conditions, IRK1 exhibited four discrete closed states with mean closed times of 0.8 ± 0.1 ms, 14 ± 0.6 ms, 99 ± 19 ms, and 2744 ± 640 ms ($n = 4$). Both the open and the three shortest closed-time constants of IRK1 decreased monotonically with membrane hyperpolarization. IRK1 open probability (P_o) decreased sharply with hyperpolarization due to an increase in the frequency of long closed events that were attributable to divalent-cation blockade. Chelation of divalent cations with EDTA eliminated the slowest closed-time distribution of IRK1 and blunted the hyperpolarization-dependent fall in open probability. In contrast, ROMK2 had shorter open and closed times and only two closed states, and its P_o was less affected by hyperpolarization. Chimeric channels were constructed to address the question of which parts of the molecules were responsible for the differences in kinetics. The property of multiple closed states was conferred by the second membrane-spanning domain (M2) of IRK. The long-lived open and closed states, including the higher sensitivity to extracellular divalent cations, correlated with the extracellular loop of IRK, including the "P-region." Channel kinetics were essentially unaffected by the N- and C-termini. The data of the present study are consistent with the idea that the locus of gating is near the outer mouth of the pore.

INTRODUCTION

Members of the inward-rectifier (Kir) family of K^+ channels share a number of basic characteristics including high selectivity for K^+ over Na^+, high P_o at the normal resting potential of the cell, and properties indicative of multi-ion occupancy of the pore (Latorre and Miller, 1983; Eisenman and Dani, 1987; Hille, 1992). However, within the inward rectifier family, there are significant differences in the single-channel conductance and in the degree of rectification (Jan and Jan, 1997; Nichols and Lopatin, 1997). The channels also exhibit a wide range of gating characteristics. In this paper we focus on the differences in the opening and closing rates of two prototypical inward rectifier K^+ channels. These are ROMK2 (Kir1.1b), a weakly rectifying channel found mainly in the kidney (Zhou et al., 1994), and IRK1 (Kir2.1), a strongly rectifying channel cloned from J774, a macrophage cell line (Kubo et al., 1993).

METHODS

Construction of chimeras

Chimeras were constructed using the splicing by overlap extension method (Horton et al., 1989). Overall schemes for each chimera are summarized in Table 1. Briefly, after the synthesis of fragment 12 and fragment 34 using polymerase chain reaction (PCR), a second PCR was conducted with primer 1, primer 4, and two fragments. The PCR product was cut with the restriction enzymes 1 and 2 to replace the corresponding parts of ROMK2 (GenBank accession No. L29403) or IRK1 (GenBank accession No. X73052). Primers (Table 2) were synthesized by Operon Technologies, Inc. (Ala-meda, CA). Nucleotide sequences between two restriction enzyme sites were checked using an ABI 377 automated DNA sequencer at The Rockefeller University DNA Technology Center (New York, NY).

Expression of channels

Plasmids were linearized with Not I restriction enzyme and transcribed in vitro with T7 RNA polymerase in the presence of the GpppG cap using the mMESSAGE mMACHINE kit (Ambion, Austin, TX). Synthetic cRNA was dissolved in water and stored at −70°C before use. Stage V–VI oocytes were obtained by partial ovariectomy of female *Xenopus laevis* (NASCO, Ft. Atkinson, WI), anesthetized with tricaine methanesulfonate (1.5 g/l, adjusted to pH 7.0). Oocytes were defolliculated by incubation in OR2 solution (82.5 mM NaCl, 2 mM KCl, 1 mM $MgCl_2$, and 5 mM HEPES, adjusted to pH 7.5 with NaOH) containing 2 mg/ml collagenase type II and 2 mg/ml hyaluronidase type II (Sigma Chemical, St. Louis, MO) for 90 min and (if necessary) another 90 min in a fresh enzyme solution at 23°C. Oocytes were injected with 0.5–1 ng of cRNA and incubated at 19°C in 2× diluted Leibovitz medium (Life Technologies, Grand Island, NY) for 1 to 4 days before measurements were made. For patch-clamp experiments, oocytes were subjected to a hypertonic shrinking solution containing 200 mM sucrose, thereby allowing the vitelline membrane to be easily removed.

Electrophysiology

Oocytes were bathed in a solution containing (in mM): KCl (110), $CaCl_2$ (2), $MgCl_2$ (1), and HEPES (5) at pH 7.4. Patch-clamp pipettes were pulled from #7052 borosilicate glass (Richland Glass Co., Richland, NJ) using a three-stage process and were coated with Sylgard. They were filled with solutions containing (in mM): KCl (110) and HEPES (5) at pH 7.4. In some cases the solution also contained 5 mM EDTA. In one set of experiments

Received for publication 29 September 1998 and in final form 27 January 1999.

Address reprint requests to Dr. Henry Sackin, Department of Physiology and Biophysics, The Chicago Medical School, 3333 Green Bay Road, North Chicago, IL 60064. Tel.: 847-578-8329; Fax: 847-578-3265; E-mail: sackinh@mis.finchcms.edu.

0006-3495/99/04/1988/16 $2.00

TABLE 1 Overall schemes for the chimeras

Chimera	Restriction Enzyme 1	Frag 12			Frag 34			Restriction Enzyme 2
		Primer 1	Template 12	Primer 2	Primer 3	Template 34	Primer 4	
Chm-1	Sal I	PI-1	IRK1	PI-20	PR-2	ROMK2	PR-10	Bgl II
Chm-4	Sal I	PI-1	Chm1	PR-24	PI-12	IRK1	PI-8	BstB I
Chm-6	Sal I	PI-1	Chm108	PR-22	PI-11	IRK1	PI-8	BstB I
Chm-7	Pst I	PR-1	ROMK2	PR-22	PI-11	Chm126	PR-10	Bgl II
Chm-8	Sal I	PI-1	IRK1	PI-21	PR-30	Chm38	PI-8	BstB I
Chm-9	Pst I	PR-1	ROMK2	PR-22	PI-17	Chm107	PR-10	Bgl II
Chm-10	Sal I	PI-1	Chm126	PR-19	PI-19	ROMK2	PI-8	BstB I
Chm-12	Sal I	PI-1	IRK1	PI-15	PR-26	Chm13	PI-8	BstB I
Chm-13	Pst I	PR-1	ROMK2	PR-17	PI-5	IRK1	PI-8	BstB I
Chm-15	Sal I	PI-1	IRK1	PI-9	PR-18	ROMK2	PR-10	Bgl II
Chm-16	Pst I	PR-1	ROMK2	PR-24	PI-12	IRK1	PI-8	BstB I
Chm-25	Sal I	PI-1	Chm1	PR-17	PI-5	IRK1	PI-8	BstB I
Chm-34	Sal I	PI-1	Chm4	PI-15	PR-26	Chm13	PI-8	BstB I
Chm-38	Sal I	PI-1	Chm15	PR-29	PI-11	IRK1	PI-8	BstB I
Chm-107	Pst I	PR-1	Chm16	PI-15	PR-26	ROMK2	PR-10	Bgl II
Chm-108	Sal I	PI-1	Chm15	PR-19	PI-19	IRK1	PI-8	BstB I
Chm-126	Sal I	PI-1	IRK1	PI-18	PR-28	ROMK2	PR-10	Bgl II

KCl was replaced by 73 mM K_2SO_4. Pipette resistances ranged from 1 to 3 MΩ. Currents were recorded with either a List EPC-7 or a Dagan 8900 patch-clamp amplifier and stored, unfiltered, on videotape. For off-line analysis, current records were replayed from videotape, filtered at 1 kHz, and sampled at 5 kHz, using an Atari-based data acquisition system (Instrutech, Mineola, NY). Construction of open- and closed-time histograms and fitting with exponential distributions were carried out using the data analysis TAC program (Sigworth and Sine, 1987). When selected records were sampled at 25 kHz rather than 5 kHz, no significant difference was found in the locations of peaks on the closed-time histograms. Hence, data were routinely sampled at 5 kHz to conserve disk space.

Data analysis

The voltage dependence of the open probability (P_o) was fit by the Boltzmann function:

$$P_o = P_{min} + \frac{1 - P_{min}}{1 + \exp\left(\frac{w - zeV}{k_B T}\right)} \quad (1)$$

where P_{min} represents the minimal P_o and w represents the conformational energy increase upon opening the channel in the absence of a membrane potential. The terms e, V, k, and T have their usual meaning.

The smooth curves in Figs. 2, 3, 7, 8, and 9 were drawn using the equations and fitted parameters enumerated in the Appendix.

RESULTS

Kinetic properties of IRK1

The basic gating characteristics of IRK1 at three different membrane potentials are shown in Fig. 1. Both openings and closures tended to be long-lived, as previously reported (Kubo et al., 1993). At a membrane potential of −100 mV (oocyte negative) the duration histogram of Fig. 1 *B* indicates that the open time is well described by a single-exponential distribution, whereas the closed times required at least four separate exponentials to fit the distribution well (Figs. 1 *C* and 6 *A*). Maximum likelihood analysis indicated that the fit with four exponentials was significantly better than the fit obtained using only three exponentials.

The voltage dependence of the kinetic parameters is illustrated in Fig. 2. The open probability (P_o) of IRK1 declined steeply as the voltage was changed from −60 mV

TABLE 2 Primers used for construction of the chimeras

Primers	5′ → 3′	Primers	5′ → 3′
PI-1	ctcagactgttttctaaagcttaaacactgg	PR-1	caggaaacagctatgaccatg
PI-5	ccttcatgtgtggtgccgtcatggcgaagatggc	PR-2	ggaggtggatgctggttgtgttcatcacagccttc
PI-8	ggtccaaagggatatactcccc	PR-10	cttgccatatatgtggctg
PI-9	gggaggtccttatgaaccagggctatcaacc	PR-17	gccatcttcgccatgacggcaccacacatgaagg
PI-11	ggcatgacttcagccttcctcttctcc	PR-18	ggttgatagccctggttcataaggacctccc
PI-12	tgtggtatgtcgtagcgtatctccatggggatct	PR-19	ccaccatgaagacagcagtggcgcactgttctgtc
PI-15	caggaaaatggcaattgggcactcg	PR-22	ggagaagaggaaggctgaagtcatgcc
PI-17	ggttacggattcaggtgtgtgacagacg	PR-24	agatccccatggagatacgctacgacatacc
PI-18	gcactgttctgtcacaaacctgaaacc	PR-26	gtgcccaattgccatttttcctgc
PI-19	gaacagtgcgccactgctgtcttcatggtgg	PR-28	ggctatggtttcaggtttgtgac
PI-20	ggctgtgatgaacacaaccagcatccacc	PR-29	ctcgtctgtcacacacctgaatccg
PI-21	gaaaacagaaaggcagccgtgaagc	PR-30	aacagcttcacggctgccttttctgttttc

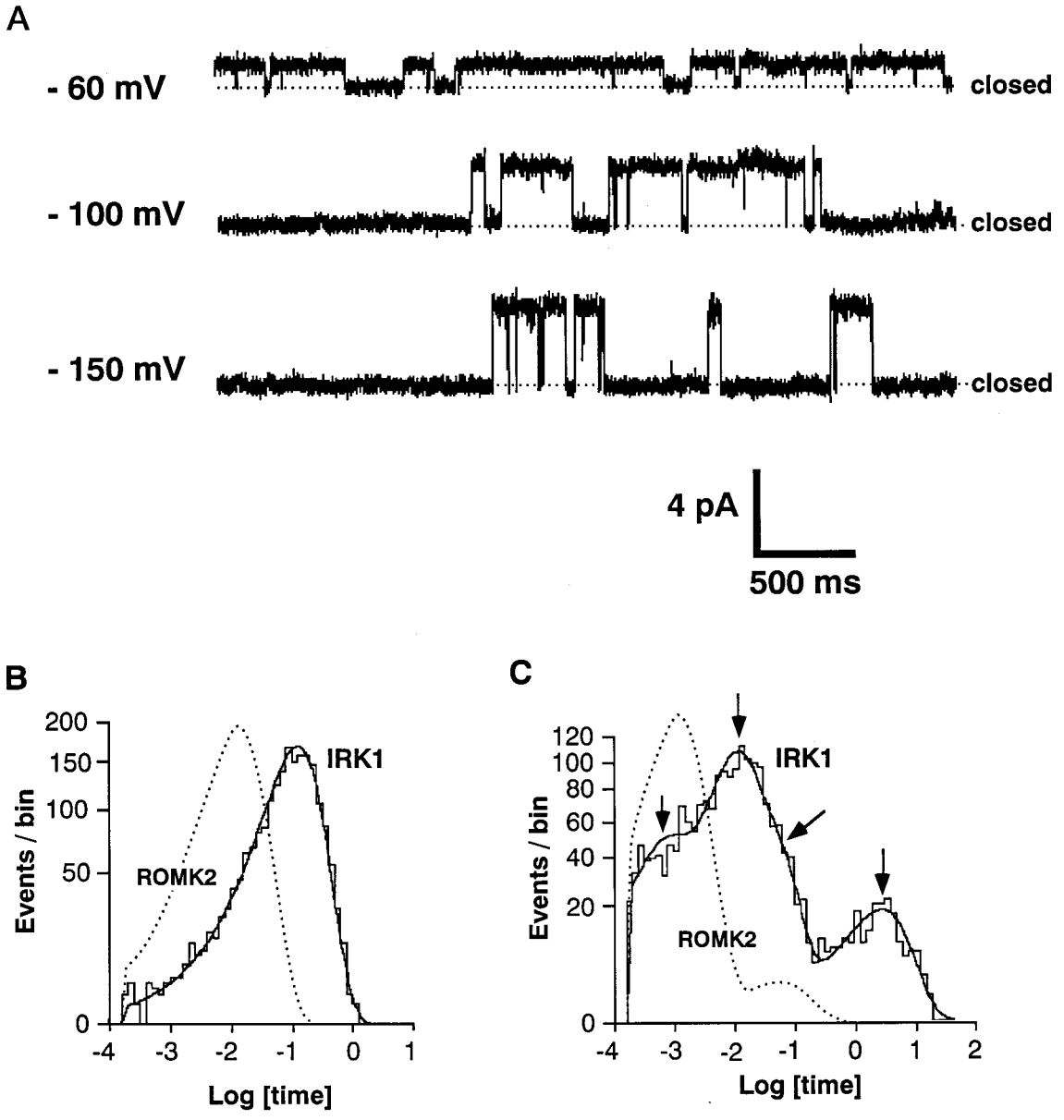

FIGURE 1 Kinetics of IRK1. No EDTA in the solutions. Currents were recorded for 45 min from a cell-attached patch containing only one channel. (*A*) Current traces of an individual IRK1 channel expressed in a *Xenopus* oocyte. Closed levels are indicated. (*B*) Open-time histogram of IRK1 at −100 mV. The solid line represents a single exponential best fit with a time constant of 131 ms. For comparison, the dotted line indicates ROMK2 open-time kinetics under similar conditions. (*C*) Closed-time histogram of IRK1 at −100 mV. The solid line represents the best fit with four exponentials having time constants of 0.6 ms (18%), 10 ms (43%), 41 ms (28%), and 2.9 s (11%). These are indicated by arrows. For comparison, the dotted line indicates ROMK2 closed-time kinetics under similar conditions.

to −150 mV (Fig. 2 *A*). This is in marked contrast to ROMK2, which exhibits little voltage dependence of open probability (*dashed line*, Fig. 2 *A*). Over the same voltage range, the mean open time of IRK1 decreased exponentially, declining e-fold for a hyperpolarization of 64 mV (*solid line*, Fig. 2 *B*). The closed-time constants of IRK1 also declined with hyperpolarization, although the longest closed time was much less sensitive to voltage than were the shorter closed times. The curves in Fig. 2 *C* were fit to the data according to Eqs. A2 and A3, given in the Appendix. Although the duration of the longest closures was not strongly affected by voltage, the number of such closures increased with hyperpolarization. This largely accounted for the substantial voltage dependence of IRK1 P_o.

Because native inward rectifiers are known to be sensitive to extracellular divalent cations (Hagiwara et al., 1978; Sakmann and Trube, 1984; Ho et al., 1993; Kubo et al., 1993; Elam and Lansman, 1995; Robertson et al., 1996), and because the kinetics of the cloned ROMK2 channel were altered by chelation of divalent cations (Choe et al., 1998), we examined the effects of adding 5 mM EDTA to the pipette solution on the gating of IRK1. As shown in

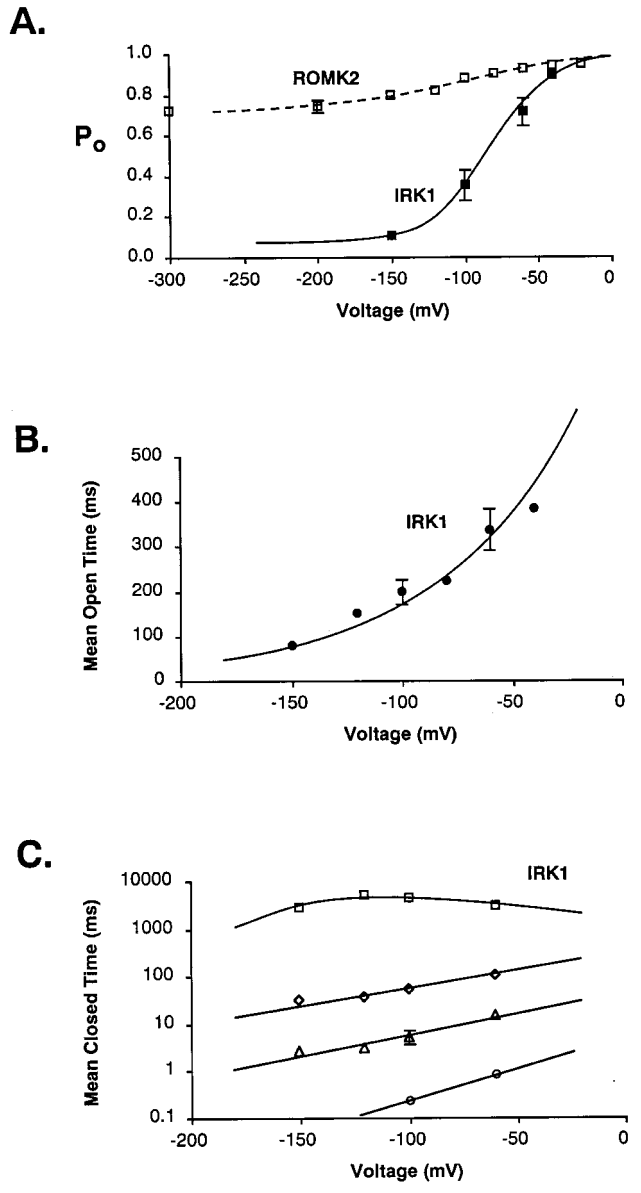

FIGURE 2 Voltage-dependence of time constants of IRK1. Data represent means ± SE for $n = 4$ IRK1 experiments. The absence of error bars on some points indicates that the SEM was obscured by the symbol. (*A*) Voltage dependence of P_o for control pipette solutions. IRK1 (*filled squares, solid line*). For comparison the P_o-*V* relationship of ROMK2 ($n = 6$) is shown on the same scale (*open squares, dashed line*). The smooth curves were drawn from Eq. 1 using the parameters given in the Appendix. (*B*) Voltage dependence of mean open times for IRK1 ($n = 4$). (*C*) Voltage dependence of mean closed times for IRK1 ($n = 4$). The four lines indicate the four discrete closed states observed with IRK1 in the absence of EDTA.

Fig. 3, long-lived closures that were prevalent under control conditions were virtually abolished by EDTA. The P_o-*V* curves associated with these experiments are shown in Fig. 3 *B*. The results of this figure strongly suggest that the reduction in P_o is a consequence of block by divalent cations, even though none were added to the control pipette solution.

To investigate the possibility that the voltage-dependent reduction in P_o arose specifically from block by trace amounts of Ba^{2+}, we repeated the measurements using 73 mM K_2SO_4 in the pipette solution. Since the solubility product of $BaSO_4$ is 1.05×10^{-10} (Weast and Selby, 1966), the ionized Ba^{2+} concentration would be <2 nM under these conditions. As shown in Fig. 3 *B*, complexation of Ba^{2+} reduced, but did not eliminate, the fall in P_o at hyperpolarizing voltages. This is consistent with reports that trace amounts of Ba^{+2} affect the gating of calcium-activated K^+ channels (Diaz et al., 1996) and ROMK2 channels (Choe et al., 1998).

Comparison of Figs. 3 *C* and 1 *B* illustrate that addition of EDTA has a relatively small effect on the mean open time of IRK1. With 5 mM EDTA in the pipette solution, the mean open time was 270 ± 26 ms ($n = 5$) at −100 mV (compared to the value of 131 ms for the experiment of Fig. 1). However, chelation of divalents virtually eliminated the longest closed time (compare Figs. 3 *D* and 1 *C*). In some experiments, the shortest closed time also disappeared (or became too short to measure) under these conditions.

Comparison with ROMK gating

Although IRK1 and ROMK2 show many structural similarities, their gating characteristics differ significantly (Chepilko et al., 1995; Choe et al., 1998). Compared to ROMK, IRK1 channels have much longer mean open times (300 ms vs. 20 ms), more resolvable closed states (four versus two under control conditions) and a stronger voltage dependence (see Fig. 2 *A*).

A major goal of this study was to investigate which aspects of the ROMK and IRK structures are responsible for these differences. To address this question we divided the primary amino acid sequence of both channels into seven different sections based on hydropathy analysis and sequence homology (Fig. 4). These are 1) the cytoplasmic N-terminal; 2) the first predicted transmembrane domain (M1); 3) the extracellular region from M1 to the P-region (MP); 4) the P-region itself containing the GYG K^+-channel signature sequence; 5) the remainder of the extracellular region from the P-region to the second predicted membrane spanning domain (PM); 6) the second predicted membrane spanning domain itself (M2); and 7) the cytoplasmic C-terminal.

The alignment of several of these regions in IRK1 and ROMK2 is shown in Fig. 4 *B*. Clearly the strongest homology is in the P-region, where 15 of 17 amino acids are identical. Significant homology also exists in M1 (7/22 identical), PM (3/8 identical) and M2 (11/22 identical). In contrast, the MP regions are quite different, as are the N- and C-termini. In Fig. 4 *B* the shaded residues comprise the putative pore helix according to the crystal structure of KcsA (Doyle et al., 1998). Chimeric molecules were constructed by combining regions from IRK1 and ROMK2, as described in the Methods section.

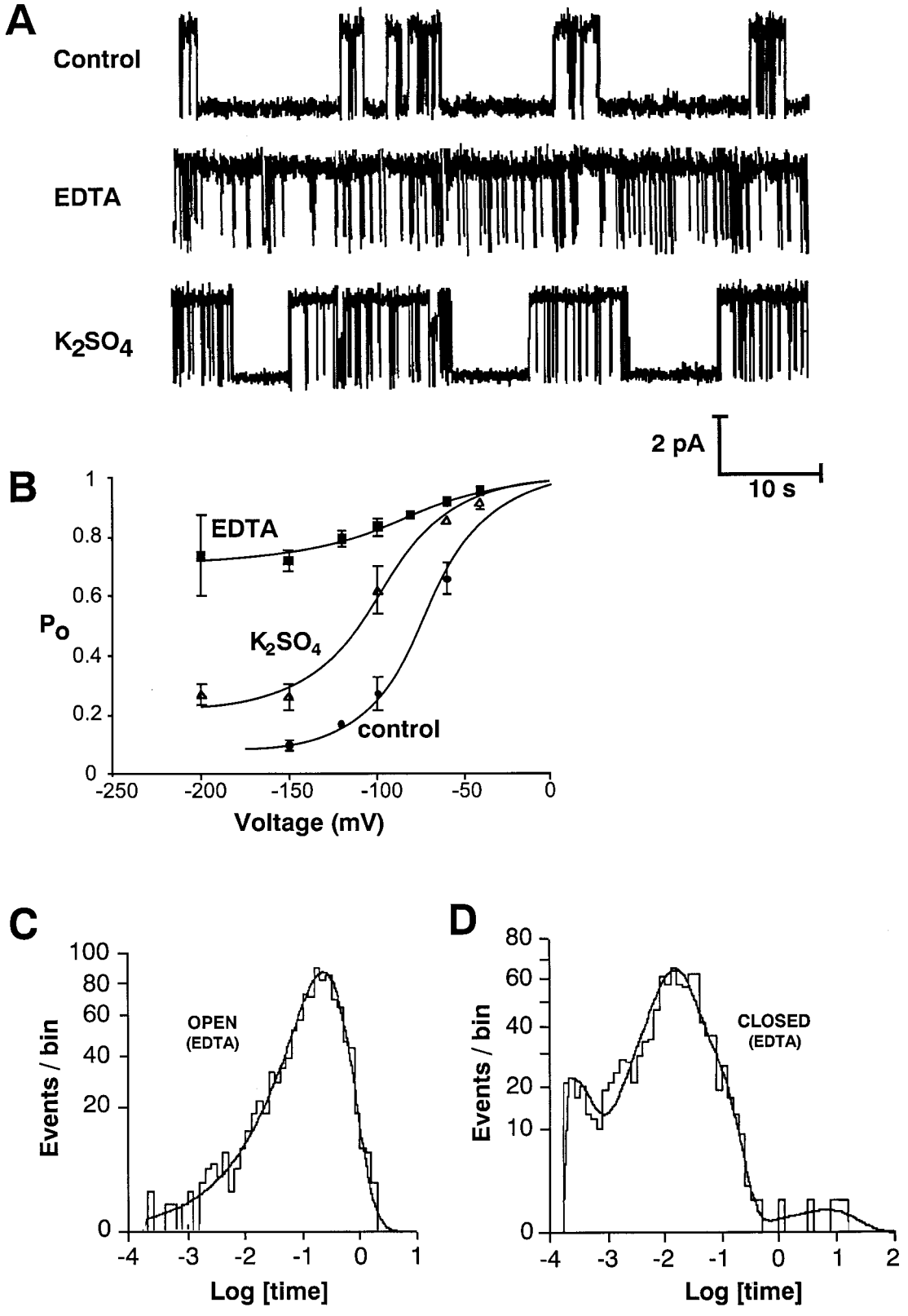

FIGURE 3 Kinetics of IRK1 after chelation of divalent cations. (*A*) Currents traces at −150 mV with control pipette solution (*top*), EDTA-containing pipette solution (*middle*), and SO_4^{2-}-containing pipette solution (*bottom*). (*B*) P_o for control pipette solution (*circles*), EDTA-containing pipette solution (*squares*), and $K_2SO_4^{2-}$-containing pipette solution (*triangles*). Data represent means ± SE for 3–6 experiments. (*C*) Open-time histogram in the presence of EDTA. The solid line represents a single exponential with a time constant of 238 ms. (*D*) Closed-time histogram in the presence of EDTA. The solid line represents the best fit with four exponnentials having time constants of 0.2 ms (20%), 13 ms (49%), 60 ms (30%), and 7.0 s (1%).

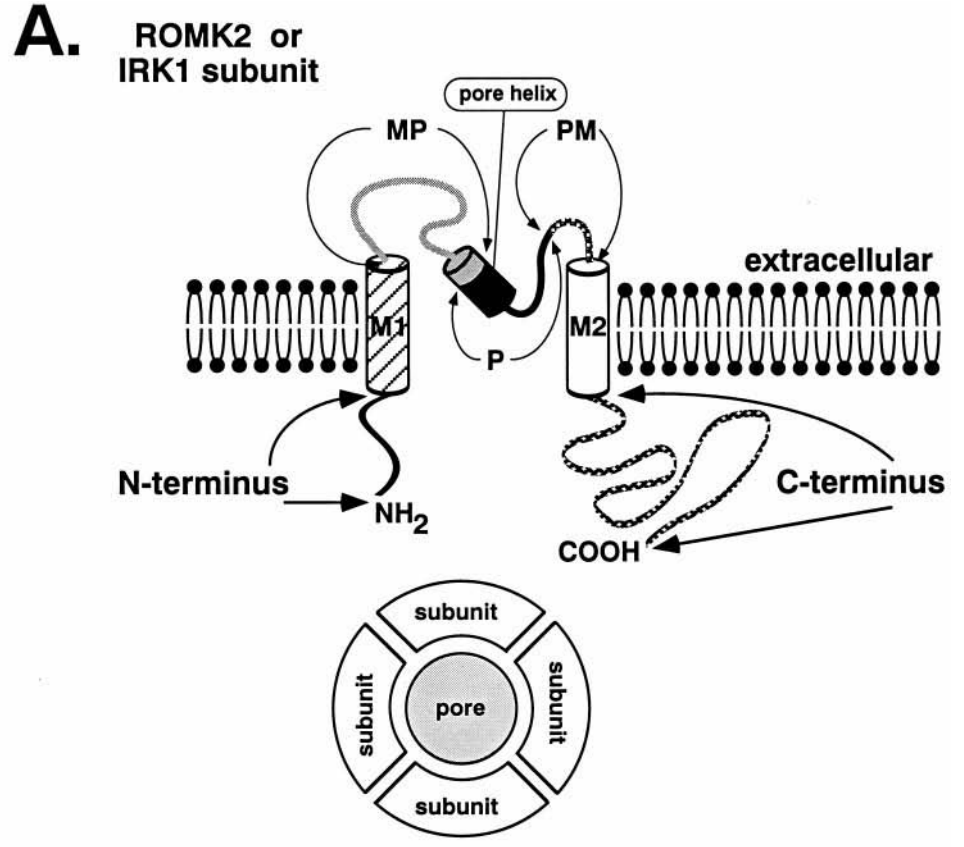

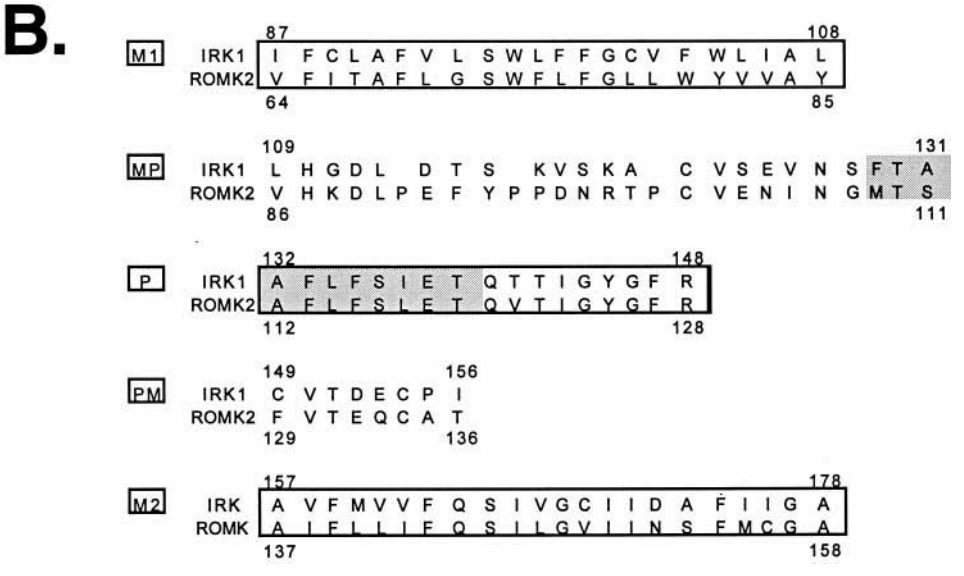

FIGURE 4 (*A*) Simplified membrane topology of ROMK and IRK subunits. M1 and M2 are membrane-spanning domains. P denotes the highly conserved domain. The segments MP and PM are, respectively, the region between M1 and P and the region between P and M2. The cylinder in the extracellular loop is the pore helix, consisting of the first half of the P region with a minor contribution from the MP region. (*B*) Specification and alignment of the different regions of IRK1 and ROMK2. Shaded residues denote the putative pore helix.

N- and C-termini do not determine gating characteristics

To examine the contribution of the cytoplasmic parts of the proteins to channel gating, we attached the N- and C-termini of IRK1 separately and together to the core component (M1, MP, P, PM, and M2) of ROMK. As indicated in Fig. 5 *A*, the kinetics of the channels changed little with substitution of these segments. In all cases, the closed-time histograms were well described by two exponentials (see below) and the open-time histograms by one exponential, similar to the case of ROMK2 channels (Chepilko et al., 1995; Choe et al., 1998). A quantitative comparison of the kinetics is shown in Fig. 5 *B*. None of the kinetic parameters were

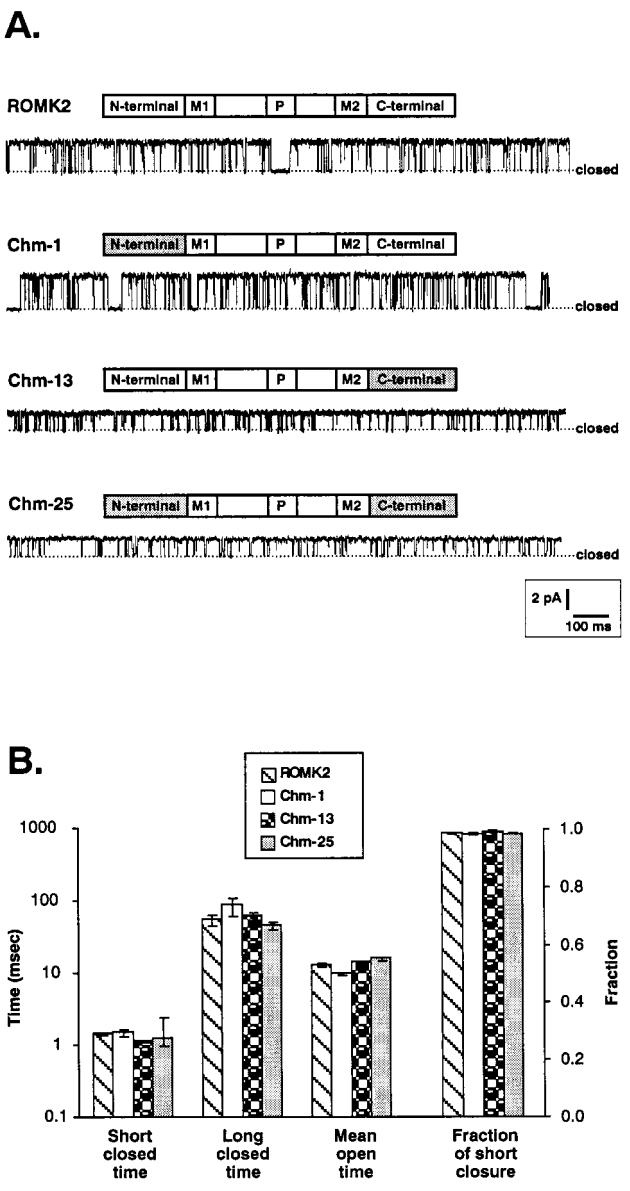

FIGURE 5 Lack of effect of N-terminus and C-terminus on ROMK gating. (*A*) Cell-attached current records obtained from the indicated chimeras, expressed in K^+-depolarized oocytes with pipette holding potential of +80 mV (oocyte −80 mV relative to pipette). Shaded rectangles correspond to IRK segments, open rectangles to ROMK2. Chm-1 and Chm-13 were constructed by replacing the N- and C-termini, respectively, with the corresponding segments from IRK1. In Chm-25 both the N- and C-termini were replaced. All chimeras display approximately the same kinetics. (*B*) Gating parameters of the chimeras shown in (*A*). Data points represent means ± SE for the following numbers of experiments: ROMK2 (n = 6), Chm-1 (n = 3), Chm-13 (n = 7), Chm-25 (n = 5).

altered significantly by changes in the cytoplasmic domains, although single-channel conductance was higher when the C-terminal region was derived from ROMK.

Multiple closed states are conferred by the M2 region

One of the striking differences between ROMK and IRK gating is that four time constants are required to fit the closed-time histograms of IRK1 (Figs. 1 *C* and 6 *A*). Only two time constants are necessary to describe ROMK kinetics over the same frequency bandwidth (Choe et al., 1998). The M2 region of IRK is essential for this difference. Substitution of only the M2 region of ROMK into the IRK channel produced a channel with gating patterns that resembled those of ROMK2 (Fig. 6 *B*). A similar result was obtained if both M1 and M2 regions of ROMK were substituted into IRK (Fig. 6 *D*). The chimera with just the M1 region of ROMK substituted into IRK also displayed altered kinetics, indicative of three discrete closed states (Fig. 6, *C* and *E*). In both chimeras Chm-108 (Fig. 6 *C*) and Chm-4 (Fig. 6 *E*), best fits to the data were obtained with three time constants (corresponding to three peaks in the distribution. Although the middle peak in Fig. 6 *E* is difficult to discern, the fitting routine gave significantly better results with three exponentials compared to two (see *inset*). In Fig. 6, *C* and *E*, the shortest closures were not observed, possibly because they were too short to be detected at the bandwidth used.

Every chimera tested in which the M2 domain was from IRK1 exhibited three or four closed states, although the values of the time constants depended on both the M1 domain and the extracellular loop (Fig. 6, *A*, *C*, and *E*). Conversely, all chimeras tested in which the M2 domain was from ROMK2 had only two closed time constants (Fig. 6, *B* and *D*). Unfortunately, chimeras with an M2 region from IRK and C-terminal region from ROMK2 were nonfunctional (Taglialatela et al., 1994; Doi et al., 1996). Hence, it was not possible to test whether having the transmembrane domains from IRK is sufficient for multiple closed states.

Closed times are affected by the extracellular region

We analyzed the closed times of those chimeras for which the closed-time distributions could be described by two exponentials, corresponding to well-defined "long" and "short" closures. All of these chimeras contained the M2 region of ROMK2, as described above. In all cases the mean durations of both short and long closures were biphasic functions of voltage, as previously described for ROMK2 itself (Choe et al., 1998).

The extracellular loop (ECL) has a major role in determining the long closed times. In Fig. 7, chimeras Chm-107 and Chm-34 were formed by respectively replacing the ROMK-ECL regions of ROMK2 and Chm-25 with the corresponding region of IRK (*shaded rectangles*). This alteration in the ECL regions increased maximum long closed times by about sixfold (Fig. 7). This was true regardless of whether the N- and C-termini were from ROMK2 (Chm-107 vs. ROMK2) or from IRK1 (Chm-34 vs. Chm-25). The closed times of all these constructs showed the same qualitative, biphasic voltage dependence, where the maximum closed time was in the range of −120 to −150 mV.

The effect of the ECL on the shorter closed times was qualitatively similar (Fig. 8). Namely, replacement of the

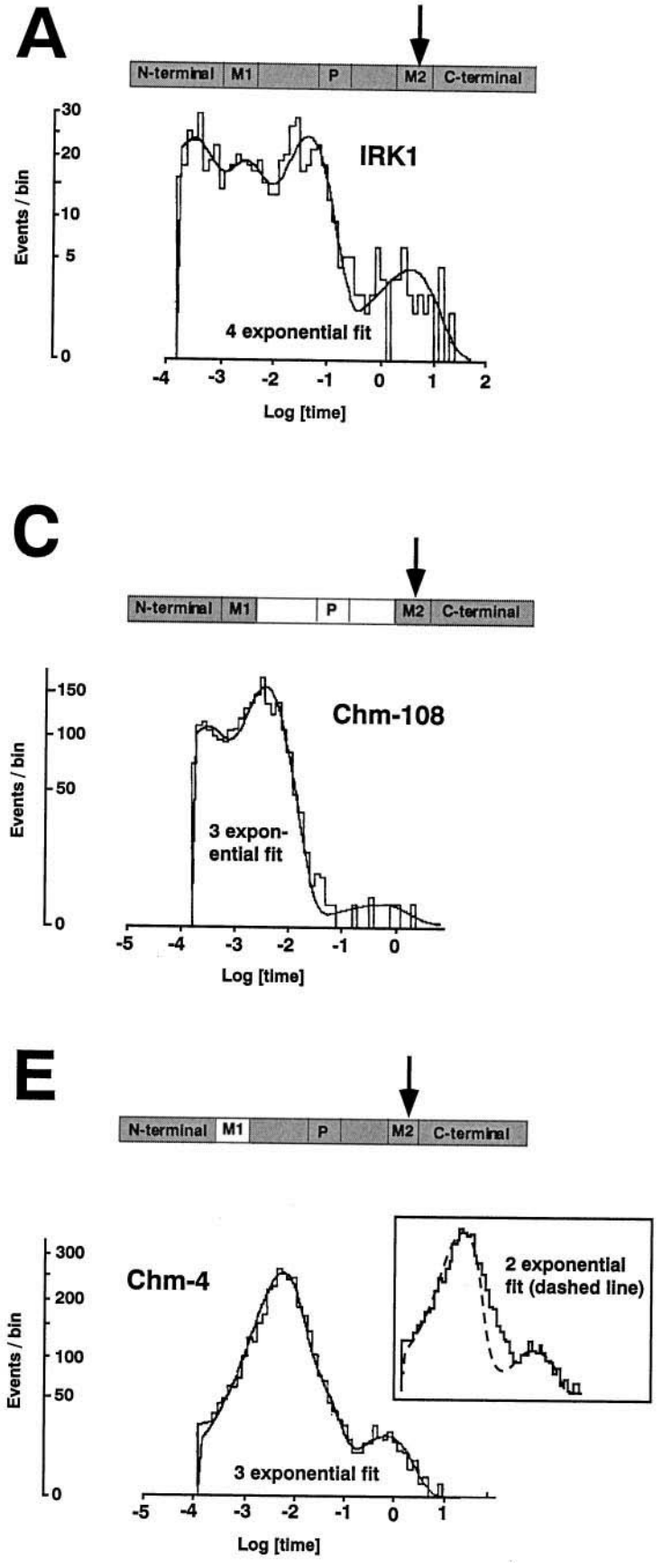

FIGURE 6 Effect of transmembrane segments on the closed-time distributions for IRK1 and chimeras, expressed in K^+-depolarized oocytes with pipette holding potential of +100 mV (oocyte −100 mV relative to pipette). Shaded rectangles correspond to IRK segments, open rectangles to ROMK2. (*A*) IRK1 with four exponentials; time constants of 0.2 ms (30%), 3 ms (25%), 47 ms (30%), and 3.7 s (6%). (*B*) Chm-12 with two exponentials; time constants of 3 ms (94%) and 144 ms (6%). (*C*) Chm-108 with three exponentials; time constants of 0.3 ms (34%), 4 ms (65%), and 530 ms (1%). (*D*) Chm-34 with two exponentials with time constants of 3 ms (96%) and 219 ms (4%). (*E*) Chm-4 with three exponentials with time constants of 8 ms (73%), 36 ms (21%), and 941 ms (6%). The inset shows that two exponentials with time constants of 11 ms (93%) and 1091 ms (7%) do not fit well.

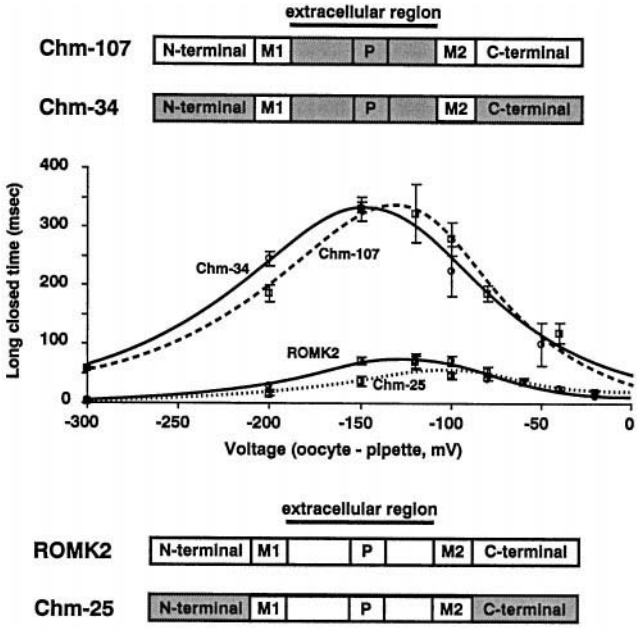

FIGURE 7 Effect of the extracellular loop on the voltage dependence of the longer closed state. Shaded rectangles correspond to segments from IRK1. Clear rectangles denote segments from ROMK2. The smooth curves were drawn from Eq. A3 using the parameters given in the Appendix. Data points represent means ± SE for the following numbers of experiments: Chm-34 (n = 3–6), Chm-107 (n = 3), ROMK2 (N = 6), Chm-25 (n = 5).

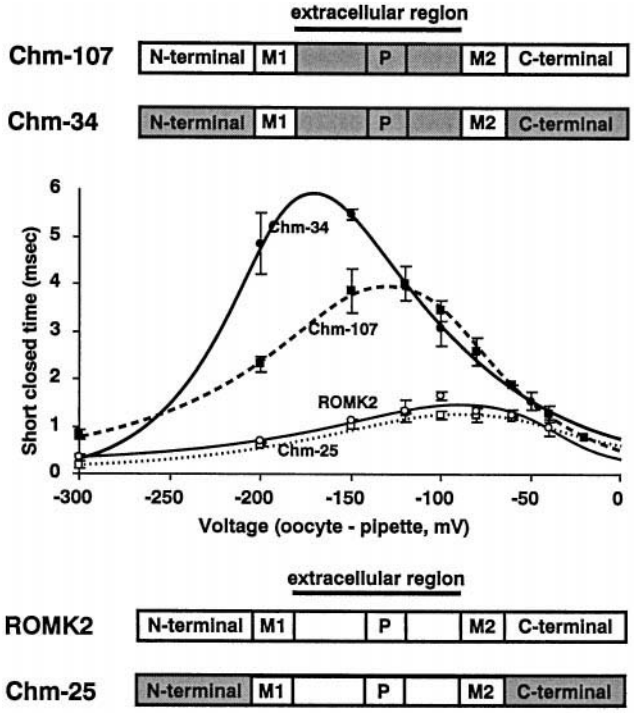

FIGURE 8 Effect of the extracellular loop on the voltage dependence of the short closed state. Shaded rectangles correspond to segments from IRK1. Open rectangles denote segments from ROMK2. The smooth curves were drawn from Eq. A3 using the parameters given in the Appendix. Data points represent means ± SE for the following numbers of experiments: Chm-34 (n = 3–6), Chm-107 (n = 3), ROMK2 (n = 6), Chm-25 (n = 5).

ROMK-ECL region by its IRK counterpart increased maximum short closed times by three to sixfold, regardless of whether the cytoplasmic parts of the channel were from IRK or from ROMK. As with the long closures, the biphasic voltage dependence of the short closures was preserved. In one case, where the transmembrane domains were from ROMK but the N- and C-termini were from IRK, there was an apparent shift in the maximum short closed time from −100 to −160 mV (Chm-34 vs. Chm-25) when the ECL was exchanged.

The ECL also determined the sensitivity of the P_o to hyperpolarization and divalent cations. As indicated in Fig. 9, chimeras having the ECL from ROMK2 had a mild dependence of P_o on voltage, similar to the ROMK2 channel itself. In contrast, when the ECL was from IRK1, there was a steep fall in P_o as the membrane was hyperpolarized from −50 to −150 mV. There was some dependence of this effect on the transmembrane domains. For example, replacement of M1 and M2 of IRK1 with the corresponding regions of ROMK2 shifted the voltage dependence by ~25 mV, but the steepness of the voltage effect was primarily a function of the ECL. As discussed above, this effect of hyperpolarization reflects interactions of divalent blocking ions with the channel. These ions probably interact directly with the extracellular portion of the channel protein.

We attempted to localize the determinants of the closed times more precisely by dividing the ECL into three regions: MP, P, and PM. As shown in Figs. 10 and 11, the main effects of the ECL on both closed times occurred with exchange of the P and PM regions. The MP region, which accounts for ~50% of the ECL, had relatively little influence on the gating parameters.

The determinants of the long and short closed times were somewhat different. For the long closures, exchanging only the P region increased the mean closed time. Exchanging the PM region had little effect by itself, but this exchange augmented the effects of the P region. In the case of the short closures, the converse pattern was seen. Exchanging only the PM region increased the duration of the short closures. Swapping only the P region had little effect, but this augmented the influence of the PM region.

Note that none of the chimeras had closures as long as those seen with IRK1 (>1 s). It therefore appears that both the transmembrane domains (at least M2) as well as the P-region and the flanking extracellular regions are involved to some extent in determining the stability of this closed state which, as suggested above, may involve the binding of divalent cations within the pore.

Open times are affected by several regions

Another significant difference between IRK1 and ROMK2 is the mean open time (Table 3). At −100 mV, the mean open time of IRK1 is ~160 ms, 10 times longer than that of ROMK2. Replacement of almost any segment of IRK from M1 to M2 with the corresponding part of ROMK2 reduced the mean open time (Table 3). The sole exception is the P

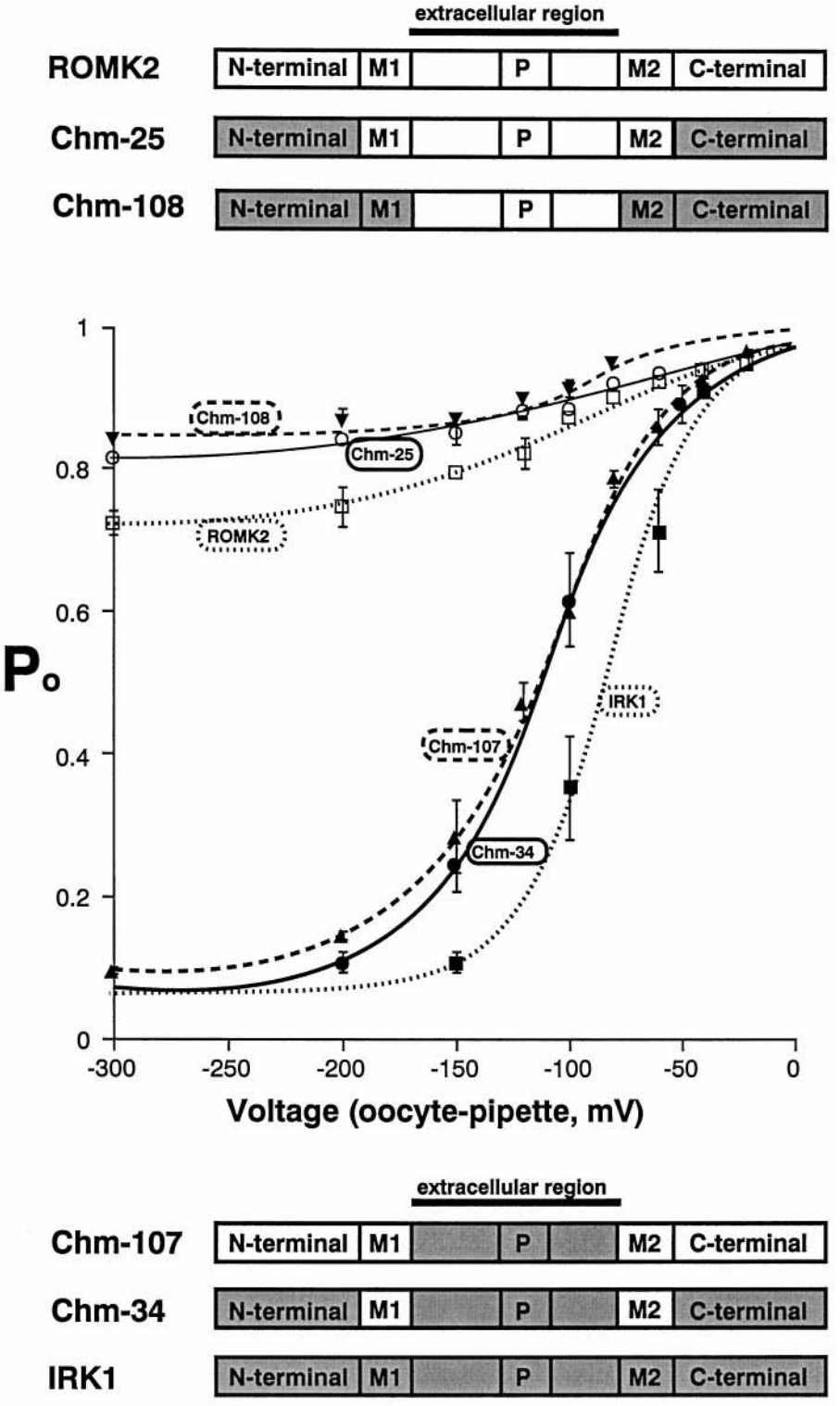

FIGURE 9 Effect of the extracellular loop on the voltage dependence of P_o. Shaded rectangles correspond to segments from IRK1. Clear rectangles denote segments from ROMK2. Chimeras in which the extracellular region was derived from ROMK2 (*top*) displayed much less sensitivity to negative membrane potential than chimeras possessing an IRK-type extracellular loop. The smooth curves were drawn from Eq. 1 using the parameters given in the Appendix. Data points represent means ± SE for the following numbers of experiments: ROMK2 (n = 6), Chm-25 (n = 3–5), Chm-108 (n = 3–4), Chm-107 (n = 3), Chm-34 (n = 3–6), IRK1 (n = 4).

region; exchange of this segment with that from ROMK2 increased the open time from 162 to 458 ms. The converse of this paradoxical effect was also observed; replacement of the P region of ROMK2 with that of IRK1 decreased the mean open time significantly (Table 4). The mean open time was most sensitive to replacement of either the PM or M2 segments of IRK by their corresponding ROMK segments (Table 3). However, the short (16 ms) open times of ROMK2 were only achieved when the entire M1-MP-P-PM-M2 region was derived from ROMK2 (Table 3).

DISCUSSION

The main conclusions of this paper are: 1) The gating properties of IRK1 differ markedly from those of ROMK2.

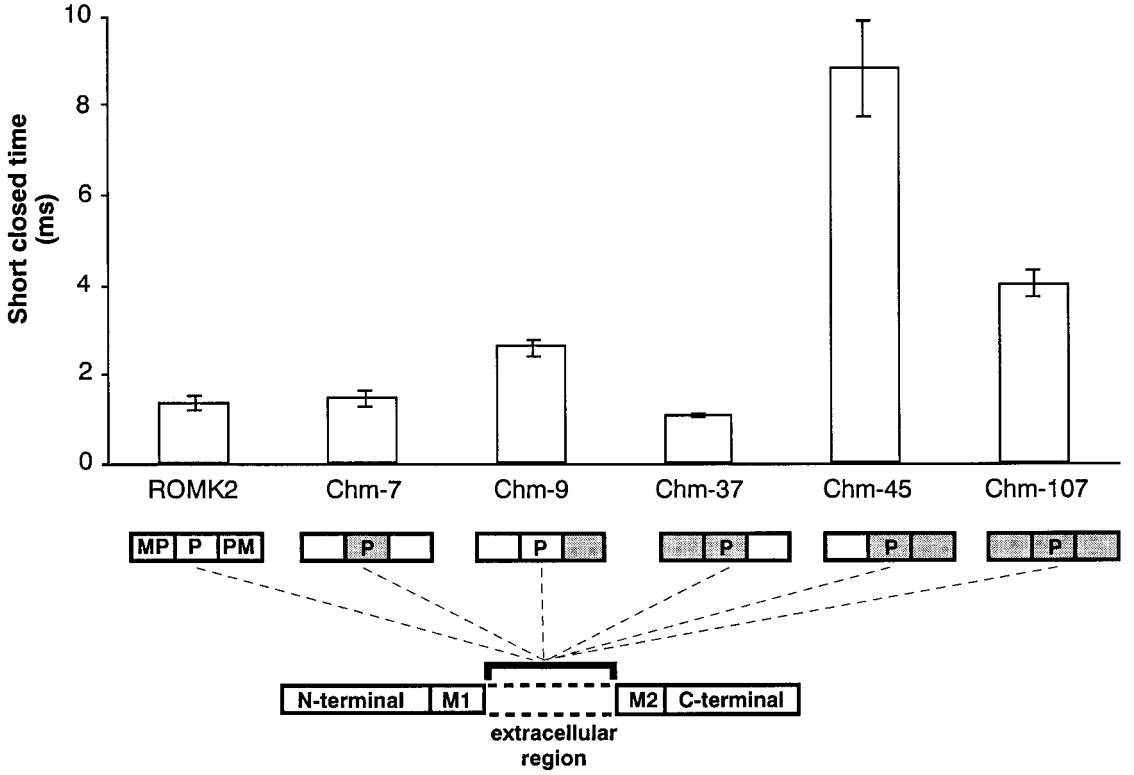

FIGURE 10 Effect of extracellular IRK segments on short closed times of chimeras at −120 mV. Shaded rectangles correspond to segments from IRK1. Open rectangles denote segments from ROMK2. Data are means ± SE for the following numbers of experiments: ROMK2 (n = 5), Chm-7 (n = 3), Chm-9 (n = 4), Chm-37 (n = 3), Chm-45 (n = 3), Chm-107 (n = 3).

The gating of IRK1 is slower, with longer mean open and closed times and four discernible closed states versus two for ROMK2. The P_o of IRK1 decreases markedly with hyperpolarization, an effect which required only trace amounts of extracellular divalent cations. 2) Channels in which the extracellular segment (MP, P, and PM in Fig. 4) was derived from IRK1 have longer open and closed times and greater sensitivity to divalent cations. 3) The number of observable closed states depends on the second membrane-spanning domain (M2), which may interact with the extracellular loop to stabilize some of the closed states.

These conclusions are discussed in more detail below.

Kinetics of IRK1

The data in Figs. 1–3 constitute, to our knowledge, the first detailed report of the kinetics of the cloned IRK1 channel. Our results are consistent with the general properties of inward rectifiers that have been previously reported (Kubo et al., 1993; Aleksandrov et al., 1996). Our results on long open times and multiple closed states are also similar to those reported for native inward rectifier channels in skeletal muscle (Matsuda and Stanfield, 1989) and aortic endothelial cells (Elam and Lansman, 1995). However, hyperpolarization decreased the closed-state lifetime for IRK1 that was expressed in oocytes, whereas it had little effect on the closed times of native inward rectifiers. We do not know the basis for this discrepancy.

The most striking features of IRK kinetics are the long open and closed times compared to ROMK. The IRK1 open times were distributed exponentially, consistent with domination of this distribution by a single open state of the channel. Similar results were obtained for native channels (Matsuda and Stanfield, 1989). The mean open time of IRK was a weak function of voltage, decreasing e-fold for a 200 mV hyperpolarization.

The closed-time distribution for IRK implied the existence of multiple closed states since at least four exponentials were required to adequately fit the data. This is clearly a minimum estimate because the kinetics of IRK1 are so slow that it was difficult to obtain recordings with enough events to resolve the histograms in greater detail than that of Fig. 6 *A*. Previous reports of native inward-rectifier channels also indicated multiple closed states (Sakmann and Trube, 1984; Matsuda and Stanfield, 1989). It has not been deter mined which of these states interact with each other or with the open state.

Similar to what was found with ROMK2 (Choe et al., 1998), the longest closed state of IRK1 probably represents block by extracellular divalent cations. Although we did not add divalents to the pipette solution, chelation of divalent

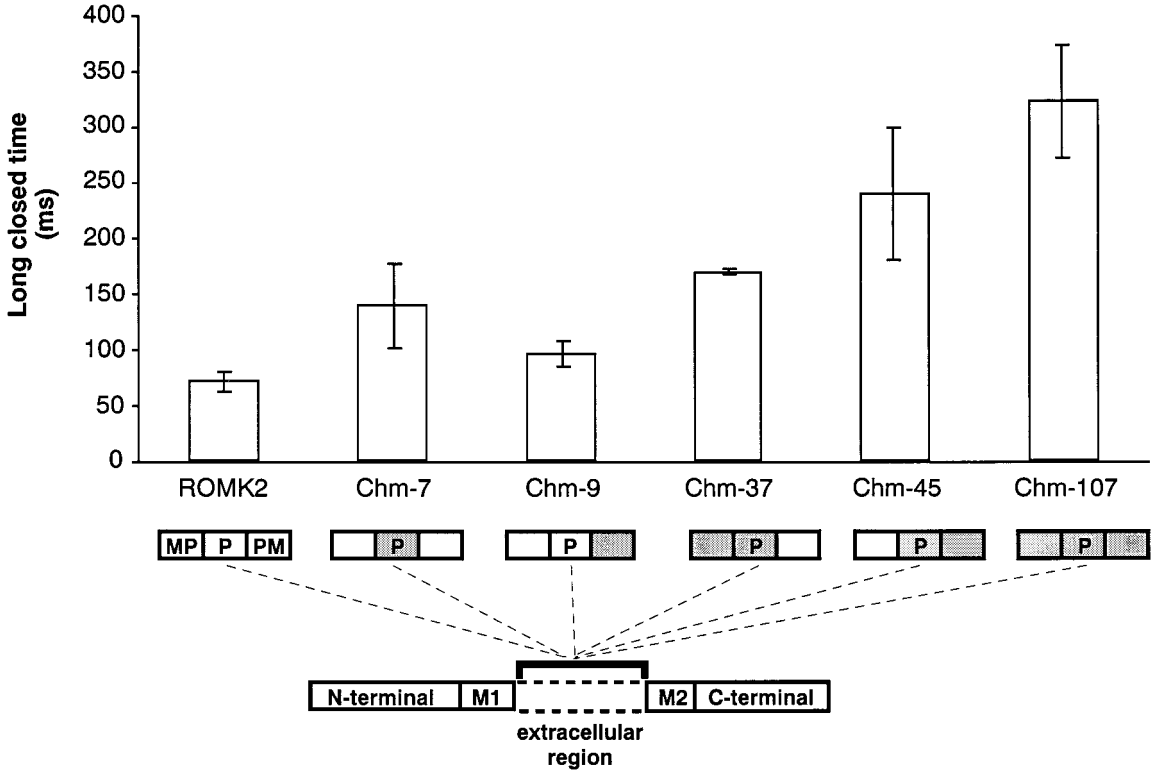

FIGURE 11 Effect of extracellular IRK segments on long closed times of chimeras at −120 mV. Shaded rectangles correspond to segments from IRK1. Open rectangles denote segments from ROMK2. Data are means ± SE for the following numbers of experiments: ROMK2 (n = 5), Chm-7 (n = 3), Chm-9 (n = 4), Chm-37 (n = 3), Chm-45 (n =3), Chm-107 (n = 3).

cations with EDTA abolished the closures longer than 1 s (Fig. 3). Reduction in Ba^{2+} concentration by precipitation with SO_4^{2-} produced a result intermediate between control and EDTA. These results imply either that there is a very high affinity site for Ba^{2+} block or that other divalent cations contribute to this phenomenon.

The source of the Ba^{2+} responsible for differences in kinetics between control and EDTA solutions was never positively identified. However, this effect of trace amounts of barium on inward rectifier kinetics was previously discussed in detail (Choe et al., 1998); where it was shown that the long closed state of ROMK2 could be attributed to the presence of 0.1 μM Ba^{2+}, an amount that might easily have come from the reagent grade KCl used to prepare the solutions.

Although much work has been done on the structural regions responsible for rectification in the K_{ir} family (Lu and MacKinnon, 1994; Taglialatela et al., 1994, 1995; Wible et al., 1994; Pessia et al., 1995; Yang et al., 1995) relatively little attention has been paid to the structural basis underlying differences in the kinetic properties of these channels. In one study using chimeras of IRK1 and GIRK1, the fast kinetics of GIRK1 could largely be attributed to its hydrophobic core (Slesinger et al., 1995). This would correspond to the M1, MP, P, PM, and M2 regions of ROMK2 or IRK1 in Fig. 4. These results are consistent with the role of the ECL region as described in the present study (Figs. 5 *A*, 7, 8, 9, and 12).

Role of the N- and C-termini

Exchanging the N- and C-termini of ROMK2 and IRK1 had negligible effect on channel kinetics under the conditions of our experiments. Since these regions share relatively little homology, one might expect to see changes in kinetics if these regions were involved in the gating process. On this basis we conclude that the cytoplasmic N- and C-termini do not participate in channel opening and closing, at least at voltages near the resting potential. However, the C-terminus is clearly involved in the Mg^{2+}-dependent closures of the channel observed at positive membrane potentials (Taglialatela et al., 1995; Yang et al., 1995).

Role of the transmembrane domains

The transmembrane domains of IRK and ROMK determine the number of closed states as well as the rates of transitions into the closed states, i.e., the mean open time. Replacement of the M2 region of IRK1 with the corresponding region of ROMK2 was sufficient to produce the basic ROMK2 kinetic pattern with two easily resolved closed states (Fig. 6). All chimeras with M2 from ROMK had two closed states,

TABLE 3 Effect of specific ROMK segments on mean open time of chimeras

Chimera		τ_{open} (ms) at –100 mV	*n*
IRK1	N-terminal M1 P M2 C-terminal	162 ± 11	4
Chm-6	N-terminal M1 P M2 C-terminal	110 ± 9	4
Chm-8	N-terminal M1 P M2 C-terminal	458 ± 6	3
Chm-10	N-terminal M1 P M2 C-terminal	45	1
Chm108	N-terminal M1 P M2 C-terminal	55 ± 2	4
Chm-4	N-terminal M1 P M2 C-terminal	65 ± 6	3
Chm-12	N-terminal M1 P M2 C-terminal	43 ± 5	3
Chm-34	N-terminal M1 P M2 C-terminal	28 ± 3	6
Chm-25	N-terminal M1 P M2 C-terminal	16 ± 1	5

whereas all chimeras having an IRK1-M2 region had more than two closed states.

In addition, replacement of the IRK1-M2 segment by its ROMK counterpart decreased mean open time by an order of magnitude (from 162 ms to 16 ms). This may be related to the associated reduction in the number of closed states. When there are rapid transitions from the open state to a single short-lived closed state, this state will dominate the closed-time histograms, making the others more difficult to resolve.

Role of the extracellular loop

IRK1 mean open time was also affected by the ECL since any chimera with a ROMK2-ECL had short open times that

TABLE 4 Effect of specific IRK segments on mean open time of chimeras

Chimera		τ_{open} (ms) at –100 mV	*n*
ROMK2	N-terminal M1 P M2 C-terminal	16 ± 1	5
Chm-1	N-terminal M1 P M2 C-terminal	11 ± 1	3
Chm-13	N-terminal M1 P M2 C-terminal	15 ± 1	7
Chm-25	N-terminal M1 P M2 C-terminal	16 ± 1	5
Chm-7	N-terminal M1 P M2 C-terminal	2 ± 0.1	3
Chm-9	N-terminal M1 P M2 C-terminal	29 ± 0.7	4
Chm-107	N-terminal M1 P M2 C-terminal	16 ± 0.6	3

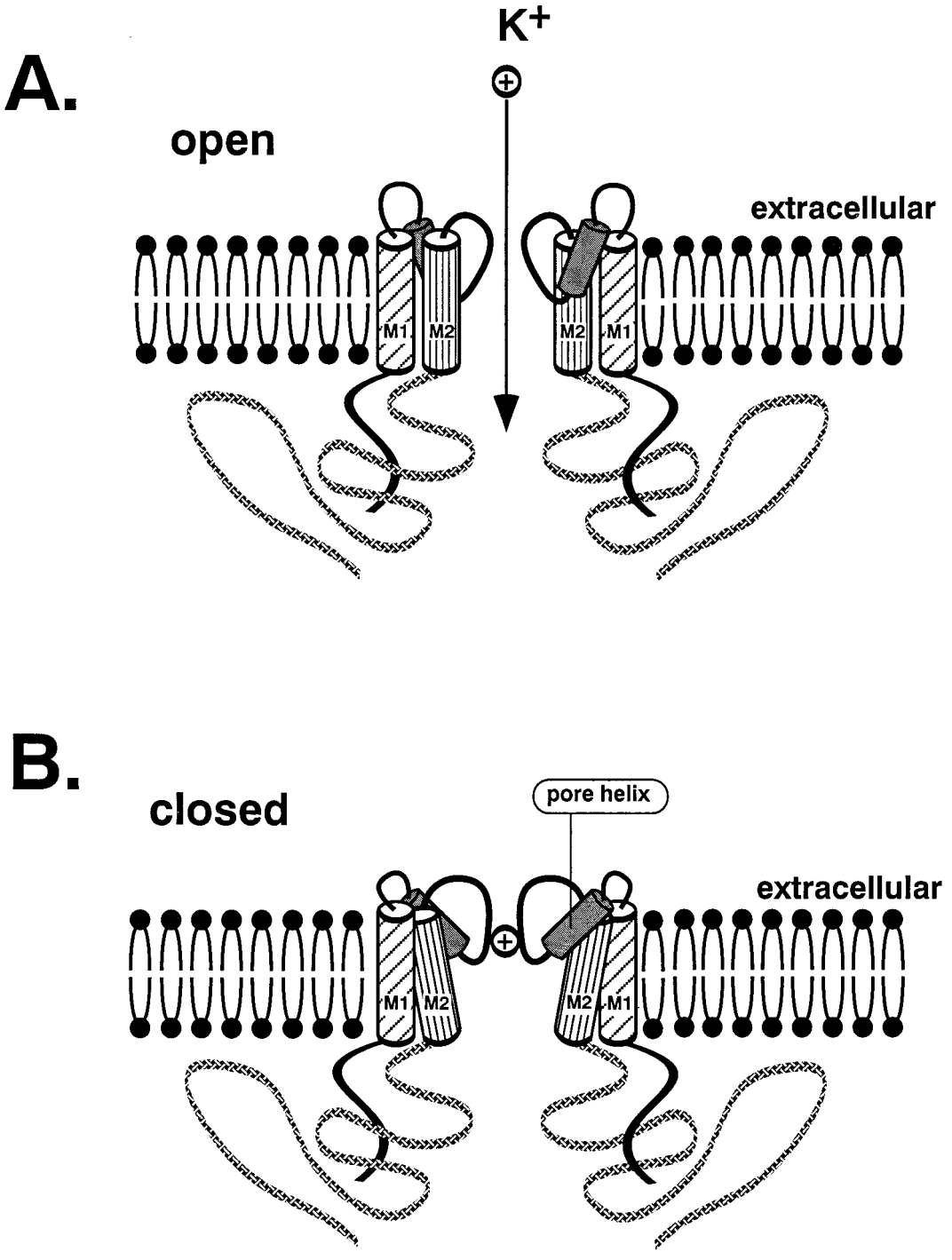

FIGURE 12 Cartoon of the gating processes for inward rectifier K^+ channels. Closure of the channel presumably involves conformational changes in the extracellular loop, and possibly the M2 transmembrane domain, since the primary structure of these regions determines the gating kinetics. The exact nature of these conformational changes is unknown. One possibility, shown here, involves a motion of the pore helices in the electric field.

were characteristic of ROMK. Thus, the long duration of the IRK1 open state appears to be determined by interactions between the M2 and ECL regions. In the absence of these interactions mean open times are short ($<$50 ms), and transitions to the short-lived closed state were frequent.

The ECL also determines the duration of closed times. For chimeras that exhibit ROMK2-like gating, with two distinct closed states, both the long and the short closed times are increased when the ECL is derived from IRK1. We previously proposed that these closed states represent block of the channel by permeant divalent and monovalent cations, respectively (Choe et al., 1998). In this hypothesis, increases in mean closed times reflect tighter binding of the blocking ions. The finding that both the long and the short closed times are

affected by the same regions of the protein support the view that these two states are closely related. The results are consistent with the idea that channel closures are the result of interactions of extracellular ions with the outer part of the conducting pore that is formed by the ECL (and stabilized by interactions with the M2 transmembrane segment).

Role of the P-region

The P-region is thought to be an important site of interaction of ions with the channel and a determinant of channel conductance and selectivity. Results of the present study implicate the P region in channel gating as well. The P regions of IRK1 and ROMK2 differ by only two amino acids: a leucine replaces an isoleucine and a valine replaces a threonine. We have previously shown that these substitutions alter the affinity of the pore for block by Ba^{2+} and by Cs^{+} (Zhou et al., 1996). The substitution also increased the frequency of the "spontaneous" long closed state of ROMK, consistent with the view that this state results from block by contaminant divalent cations, probably Ba^{2+}.

Although the duration of the short closed states was not dramatically changed by this substitution, the rate of occurrence of the short closures was increased in those chimeras having an IRK P-region. In terms of the previous model, this might represent either an increase in the occupancy of a monovalent binding site by K^{+} or an increase in the probability of induction of a deeper energy well to trap permeant ions (Choe et al., 1998).

SUMMARY

Fig. 12 is a cartoon of the gating process, based on data from the present study as well as earlier work (Choe et al., 1998). The GYG selectivity site of the channel may be stabilized in a relatively rigid configuration by hydrogen bonding and van der Waals interactions (Doyle et al., 1998). However, the inner region of the pore could be flexible enough to interact dynamically with permeant ions (Fig. 12 *B*). In this model, long closures are due to a high-affinity binding of permeant divalents such as Ba^{2+}, whereas short closures involve a conformational change of the inner P region, correlated with the presence of a permeant monovalent ion within the pore. This involves the coordinate movements of the P, PM, and M2 regions, although the exact nature of this interaction between protein and permeant ion is unknown. One possibility is a movement of the pore helix, which sits at an angle to the plane of the membrane (Doyle et al., 1998). Because an α-helix has an associated macro dipole (Hol, 1985) it will feel a torque in the presence of an electric field. Voltage-dependent changes in the position of this and associated parts of the protein could constrict the pore, transiently trapping a permeating ion and producing a channel closure.

The IRK1 clone was a generous gift of Dr. William Thornhill (Mt. Sinai School of Medicine).

This work was supported by National Institutes of Health Grants DK46950 (to H.S.) and DK27847 (to L.G.P.).

APPENDIX

The data of Figs. 2 *A*, 3 *B*, and 9 were fit to Eq. 1 of the text:

$$P_o = P_{min} + \frac{1 - P_{min}}{1 + \exp\left(\frac{w - zeV}{k_B T}\right)} \quad \text{(A1)}$$

The data of Figs. 2 *B* and *C* and 7 and 8 were fit to generalized forms for open and closed times based on equations developed in Choe et al., 1998:

$$\tau_o = A \cdot \exp\left(B \frac{eV}{k_B T}\right) \quad \text{(A2)}$$

$$\tau_c = \left\{A \cdot \exp\left(B \frac{eV}{k_B T}\right) + C \cdot \exp\left(D \frac{eV}{k_B T}\right)\right\}^{-1} \quad \text{(A3)}$$

or

$$\tau_c = E \cdot \exp\left(F \frac{eV}{k_B T}\right) \quad \text{(A4)}$$

FIG 2 A: The best-fit values used to construct the curves of Fig. 2 *A* were:

	z	$w/(k_B T)$	P_{min}
ROMK2 (open squares)	0.54	−2.3	0.72
IRK1 (filled squares)	1.3	−3.6	0.08

Fig 2 *B*: The solid line in Fig. 2 *B* was constructed according to Eq. A2, where the best-fit parameters were:

	A	B
τ_o (IRK1)	826	0.4

Fig 2. *C*: The solid lines in Fig. 2 *C* were constructed according to Eqs. A3 and A4, where the best-fit parameters were from longest (top) to shortest (bottom):

?	A	B	C	D	E	F
τ_{c1} (IRK1)	1.06	0.45	0.002	−0.86		
τ_{c2} (IRK1)					219	0.3
τ_{c3} (IRK1)					27	0.3
τ_{c4} (IRK1)					2.2	0.4

FIGURE 3 B: The P_o data of Fig 3 *B* were fit by Eq. 1 of the text. The best-fit values used to construct the curves were:

	z	$w/(k_B T)$	P_{min}
Control	1.3	−3.6	0.08
EDTA	0.8	−2.9	0.71
$K_2SO_4^{2-}$	1.2	−4.5	0.22

FIGURE 7: The long closed-time constant data were fit to Eq. A3, where the best-fit parameters were:

	A	B	C	D	# of expt.
τ_c (Chm-34)	22	0.02	0.19	−0.02	3 to 6
τ_c (Chm-107)	32	0.03	0.34	−0.01	3
τ_c (ROMK2)	92	0.02	0.51	−0.02	5 to 9
τ_c (Chm-25)	76	0.02	0.83	−0.02	3 to 4

FIGURE 8: In Fig 8, the short closed-time constant data were fit to Eq. A3, where the best-fit parameters were:

	A	B	C	D	# of expt.
τ_c (Chm-34)	1327	0.01	0.19	−0.03	3 to 6
τ_c (Chm-107)	2042	0.03	35	−0.01	3
τ_c (ROMK2)	2858	0.03	249	−0.01	5 to 9
τ_c (Chm-25)	1542	0.02	158	−0.01	3 to 4

FIGURE 9: In Fig. 9, the P_o data of Fig. 3 *B* were fit by Eq. 1 of the text. The best-fit values used to construct the curves were:

	z	$w/(k_BT)$	P_{min}
Chm-108	1.0	−4.0	0.85
Chm-25	0.4	−1.5	0.81
ROMK2	0.54	−2.3	0.72
Chm-107	0.9	−3.8	0.1
Chm-34	0.9	−3.8	0.07
IRK1	1.3	−3.5	0.08

REFERENCES

Aleksandrov, A., B. Velimirovic, and D. E. Clapham. 1996. Inward rectification of the IRK1 K^+ channel reconstituted in lipid bilayers. *Biophys. J.* 70:2680–2687.

Chepilko, S., H. Zhou, H. Sackin, and L. G. Palmer. 1995. Permeation and gating properties of a cloned renal K^+ channel. *Am. J. Physiol*. 268: C389–C401.

Choe, H., H. Sackin, and L. G. Palmer. 1998. Permeation and gating of an inwardly rectifying potassium channel: evidence for a variable energy well. *J. Gen. Physiol.* 112:433–446.

Diaz, F., M. Wallner, E. Stefani, L. Toro, and R. Latorre. 1996. Interaction of internal Ba^{2+} with a cloned Ca(2+)-dependent K+ (hslo) channel from smooth muscle. *J. Gen. Physiol*. 107:399–407.

Doi, T., B. Fakler, J. H. Schultz, U. Schulte, U. Brandle, S. Weidemann, H. P. Zenner, F. Lang, and J. P. Ruppersberg. 1996. Extracellular K^+ and intracellular pH allosterically regulate renal Kir1.1 channels. *J. Biol. Chem*. 271:17261–17266.

Doyle, D. A., J. M. Cabral, R. A. Pfuetzner, A. Kuo, J. M. Gulbis, S. L. Cohen, B. T. Chait, and R. MacKinnon. 1998. The structure of the potassium channel: molecular basis of K^+ conduction and selectivity. *Science*. 280:69–77.

Eisenman, G., and J. A. Dani. 1987. An introduction to molecular architecture and permeability of ion channels. *Annu. Rev. Biophys. Biophys. Chem*. 16:205–226.

Elam, T. R., and J. B. Lansman. 1995. The role of Mg^{2+} in the inactivation of inwardly rectifying K^+ channels in aortic endothelial cells. *J. Gen. Physiol*. 105:463–484.

Hagiwara, S., S. Miyazaki, W. Moody, and J. Patlak. 1978. Blocking effects of barium and hydrogen ions on the potassium current during anomalous rectification in the starfish egg. *J. Physiol*. 279:167–185.

Hille, B. 1992. Ionic Channels of Excitable Membranes. Sinauer Assoc., Sunderland, MA. (2nd edition).

Ho, K., C. G. Nichols, W. J. Lederer, J. Lytton, P. M. Vassilev, M. V. Kanazirska, and S. C. Hebert. 1993. Cloning and expression of an inwardly rectifying ATP-regulated potassium channel. *Nature* 362: 31–38.

Hol, W. G. J. 1985. The role of the α-helix dipole in protein function and structure. *Prog. Biophys. Mol. Biol.* 45:149–195.

Horton, R. M., H. D. Hunt, S. N. Ho, J. K. Pullen, and L. R. Pease. 1989. Engineering hybrid genes without the use of restriction enzymes: gene splicing by overlap extension. *Gene*. 77:61–68.

Jan, L. Y., and Y. N. Jan. 1997. Cloned potassium channels from eukaryotes and prokaryotes. *Annu. Rev. Neurosci*. 20:91–123.

Kubo, Y., T. J. Baldwin, Y. N. Jan, and L. Y. Jan. 1993. Primary structure and functional expression of a mouse inward rectifier potassium channel. *Nature* 362:127–133.

Latorre, R., and C. Miller. 1983. Conduction and selectivity in potassium channels. *J. Membr. Biol*. 71:11–30.

Lu, Z., and R. MacKinnon. 1994. Electrostatic tuning of Mg^{2+} affinity in an inward-rectifier K^+ channel. *Nature*. 371:243–246.

Matsuda, H., and P. R. Stanfield. 1989. Single inwardly rectifying potassium channels in cultured muscle cells from rat and mouse. *J Physiol. (Lond.)*. 414:111–124.

Nichols, C. G., and A. N. Lopatin. 1997. Inward rectifier potassium channels. *Annu. Rev. Physiol*. 59:171–191.

Pessia, M., C. T. Bond, M. P. Kavanaugh, and J. P. Adelman. 1995. Contributions of the C-terminal domain to gating properties of inward rectifier potassium channels. *Neuron*. 14:1039–1045.

Robertson, B. E., A. D. Bonev, and M. T. Nelson. 1996. Inward rectifier K^+ currents in smooth muscle cells from rat coronary arteries: block by Mg^{2+}, Ca^{2+}, and Ba^{2+}. *Am. J. Physiol*. 271: H696–H705.

Sakmann, B., and G. Trube. 1984. Voltage-dependent inactivation of inward-rectifying single-channel currents in the guinea-pig heart cell membrane. *J. Physiol. (Lond.)*. 347:659–683.

Sigworth, F. J., and S. M. Sine. 1987. Data transformations for improved display and fitting of single-channel dwell time histograms. *Biophys. J*. 52:1047–1054.

Slesinger, P. A., E. Reuveny, Y. N. Jan, and L. Y. Jan. 1995. Identification of structural elements involved in G protein gating of the GIRK1 potassium channel. *Neuron*. 15:1145–1156.

Taglialatela, M., E. Ficker, B. A. Wible, and A. M. Brown. 1995. C-terminus determinants for Mg^{2+} and polyamine block of the inward rectifier K^+ channel IRK1. *Embo J*. 14:5532–5541.

Taglialatela, M., B. A. Wible, R. Caporaso, and A. M. Brown. 1994. Specification of pore properties by the carboxyl terminus of inwardly rectifying K^+ channels. *Science*. 264:844–847.

Weast, R. C., and S. M. Selby. 1966. Handbook of Chemistry and Physics. The Chemical Rubber Co., Cleveland, OH.

Wible, B. A., M. Taglialatela, E. Ficker, and A. M. Brown. 1994. Gating of inwardly rectifying K^+ channels localized to a single negatively charged residue. *Nature*. 371:246–249.

Yang, J., Y. N. Jan, and L. Y. Jan. 1995. Control of rectification and permeation by residues in two distinct domains in an inward rectifier K^+ channel. *Neuron*. 14:1047–1054.

Zhou, H., S. Chepilko, W. Schutt, H. Choe, L. G. Palmer, and H. Sackin. 1996. Mutations in the pore region of ROMK enhance Ba^{2+} block. *Am. J. Physiol*. 271:C1949–C1956.

Zhou, H., S. S. Tate, and L. G. Palmer. 1994. Primary structure and functional properties of an epithelial K^+ channel. *Am. J. Physiol*. 266: C809–C824.